



EGYPTIAN ACADEMIC JOURNAL OF
BIOLOGICAL SCIENCES
ZOOLOGY

B

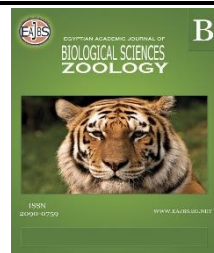


ISSN
2090-0759

WWW.EAJBS.EG.NET

Vol. 14 No. 2 (2022)

www.eajbs.eg.net



1-Preparation, Characterization, and Efficiency of Loading *Leiurus quinquestriatus* Venom on Chitosan Nanoparticles Extracted from Some Scorpions

Mostafa A. El-Sheikh*, Ahmed Badry, Mohamed Abdelaal and Ahmed Abd El-Aziz

Zoology Department, Faculty of Science, Al-Azhar University, Cairo, Egypt

E-mail*: MostafaAbdEl-hafeez.201@azhar.edu.eg

ARTICLE INFO

Article History

Received:3/9/2022

Accepted:6/11/2022

Available:12/11/2022

Keywords:

Scorpion venom, chitosan, chitosan nanoparticles, ionic gelation.

ABSTRACT

Aim: This investigation aims to extract chitin and chitosan from the three scorpions: *Leiurus quinquestriatus* (LQ), *Androctonus crassicauda* (AC) and *Androctonus amoreuxi* (AA) for the first time and to determine the loading capacity and efficiency of LQ venom-loaded chitosan nanoparticles (V-CN). **Methods:** chitin was extracted and converted to chitosan which is converted to nanoparticles (Cs-NPs) by ball-milling technique. LQ venom was collected, characterized, and loaded on Cs-NPs via the ionic gelation method. Different techniques were used to characterize the obtained compounds. **Results:** the dried powder of LQ, AC, and AA contained 19.7 %, 15.4 %, and 15 % chitin, respectively. FT-IR confirmed the successful preparation of chitin, chitosan, and V-CN samples. Loading capacity reached 76.50 %, while encapsulation efficiency reached 87.98 %. **Conclusion:** scorpion venom was effectively loaded on chitosan samples. Its physical and compound qualities, specifically, were viewed as great for biomedical and drug applications.

INTRODUCTION

Roughly 2581 scorpion species were recorded all over the world, except in Antarctica (Alqahtani and Badry, 2021). Just about 1500 scorpion species are avowed in the Buthidae grounding, of which, unaccompanied 50 species are harmful to humans (Abd El-Aziz *et al.*, 2019). Scorpions' morphology did not vary much amongst specific species, except for each form and length in their chela (pincers), which are placed on the end of pedipalps (Kellersztein *et al.*, 2019). Only three publications had been affectionate to the structure and dowry of the superficial disposition or cuticle of scorpions all over the world (Krishnan, Ramachandran and Santanam, 1955; Kaya, Asan-Ozusaglam and Erdogan, 2016; Kellersztein *et al.*, 2019).

Chitin is an ample mucopolysaccharide, white, difficult, inelastic, nitrogenous compound, the by-product of the fishery enterprise, it is the tabled after cellulose in terms of abundance (Gopakumar *et al.*, 2018). The shells of crustaceans including shrimp, crabs, and lobster are the primary providers of chitin (Fernando *et al.*, 2021). Chitin is likewise discovered in the exoskeleton of mollusks, insects, and arachnids which include scorpions as well as in the cellular partitions of a few fungi (Fernando *et al.*, 2021).

Chitosan is non-poisonous, biodegradable, bioadhesive polysaccharide and hydrophilic chitosan nanoparticle that stands out for the conveyance of restorative peptides, proteins, antigens, oligonucleotides, and qualities by intravenous, oral, and mucosal organizations (Hao *et al.*, 2021 and Sivanesan *et al.*, 2021). Chitosan is broadly utilized in drug research and the business as a transporter for drug conveyance and as a biomedical material (Heller *et al.*, 2013). Chitosan is combined utilizing its parent polymer chitin by the deacetylation technique, chitosan is liked in bio-applications habitually (Islam, Bhuiyan and Islam, 2017 and M, 2017). Chitosan enjoys many benefits, especially while creating nanoparticles; among these, are its capacity to control the arrival of dynamic specialists, aversion to the utilization of dangerous natural solvents while manufacturing particles, its cationic nature, and its mucoadhesive person which increments remaining time at the site of ingestion (Islam, Bhuiyan and Islam, 2017).

For insurance and prey catch, the venom apparatus of scorpions produce venom, which is a combination of proteins (synthetics and peptides) and non-proteins like inorganic salts, lipids, nucleotides, free amino acids, and water-based compounds (Gopalakrishnakone *et al.*, 2015 and Elrayess *et al.*, 2022).

Most of the peptides in scorpion venom are disulfide and non-disulfide spread over, and a few of them have been displayed to have hostile to epileptic, hemolytic, against thrombotic, relieving, antibacterial, and anticancer properties (Elrayess *et al.*, 2022; Mishal *et al.*, 2013; Ortiz *et al.*, 2015; Attarde and Pandit, 2016; Salem *et al.*, 2016; Tobassum *et al.*, 2018; Shah *et al.*, 2018; Akef, 2019; Ahmadi *et al.*, 2020; Díaz-García and Varela, 2020).

Intriguingly, the objective of this work was to extract chitin for the inaugural time from the cuticle of three scorpions: *Leiurus quinquestriatus*, *Androctonus crassicauda*, and *Androctonus amoreuxi*, to prepare chitosan from chitin, and to convert chitosan physically, to chitosan nanoparticles using the ball-milling technique. The study also aimed to chemically stack the venom of only one scorpion on chitosan samples to prepare venom-loaded chitosan nanoparticles and assess their physicochemical properties.

MATERIALS AND METHODS

Scorpions Collection:

Firstly, a total of 53 scorpions from three species: 24 from *Leiurus quinquestriatus* (LQ), 16 from *Androctonus crassicauda* (AC), and 13 from *Androctonus amoreuxi* (AA) were collected from some localities in Egypt, will be mentioned later. The identification of scorpions was carried out according to (Coelho *et al.*, 2017; Saleh *et al.*, 2017; Abd El-Aziz *et al.*, 2019). Scorpions were preserved in 70% ethyl alcohol. For obtaining the venom, only *Leiurus quinquestriatus* species (LQ) was used. In this experiment, 300 other scorpion specimens (LQ) were obtained.

The experiments comply with the arrival guidelines and are carried out following the National Research Council's Guide for the care and use of laboratory animals.

Leiurus quinquestriatus: One of the most well-known and restoratively significant scorpion species in Egypt. It is known as the yellow scorpion. Its geological conveyance has been limited to Egypt and Sudan. It is a medium size scorpion animal category, the complete length is somewhere in the range of 9.0 and 9.5 cm, and its shading is orangish-yellow. Prosomal carapace and metasomal portion 5 with a dark color. It has lengthened the chela. The vesicle has a yellow tone with a reddish-brown colored aculeus toward the end (Coelho *et al.*, 2017; Saleh *et al.*, 2017; Abd El-Aziz *et al.*, 2019). The current samples were collected from Aswan and Nasser Lake regions. The average weight of this scorpion was 1.07 ± 0.22 g.

***Androctonus crassicauda*:**

This species is recorded in Sinai. It is known as the Arabian fat-tailed scorpion. The shading of this species is for the most part dark with a length going somewhere in the range of 10.0 and 11.5 cm. There is a slender pedipalp with a large chela. Reversible metasomal segments are marginally bigger, and carinae have decidedly developed. Vesicles have three series of granules, each with a reasonably bowed aculeus (Coelho *et al.*, 2017; Saleh *et al.*, 2017; Abd El-Aziz *et al.*, 2019). The present samples were collected from Wadi Fieran and Sant Katherine, South Sinai. The average weight of this scorpion was 1.61 ± 0.27 g.

***Androctonus amoreuxi*:**

It is known as the yellow fat-tailed scorpion. This species is immense, arriving at a length of 10.0 cm. The variation has prosomal carapace and tergites that are primarily yellow. Yellowish metasomal segments have a predictable width while looking in reverse. The vesicle has a blushing, dark aculeus toward the start and a ground that is yellowish. The vesicle is perceptibly more modest than the aculeus (Coelho *et al.*, 2017; Saleh *et al.*, 2017; Abd El-Aziz *et al.*, 2019). The current samples were collected from Dakhla Oasis, Al-Wadi El-Jadid Governorate. The average weight of this scorpion was 1.96 ± 0.19 g.

Extraction and Characterization of Chitin:

Specimens of scorpions were cleaned and dried for a lot of time at the surrounding temperature (two months). Just the interior viscera were eliminated, and the exoskeleton and tail were gauged. The items were mixed with an electric blender (Moulinex-450 wat-1.5 litter, LM242025, France) and squashed with a mortar to make powders that pass a 300-micron strainer. Seclusion of chitin from scorpions included three conventional advances: deproteinization [the process was rehashed a few times for three days until the absence of color in the medium which represented the absence of protein], demineralization, and decolorization. These steps were completed for every species, independently utilizing the technique depicted by Sagheer *et al.* (2009). Fig. 1 showed a schematic portrayal of the development of chitin from the three scorpions (LQ, AC, and AM), the various results of chitin samples were coded as CH1, CH2 and CH3, separately. Chitin tests were described by the dissolvability test as described by Hassan, Mohamed and Taher (2016); Roy *et al.* (2017); Ou *et al.* (2018); Taher *et al.* (2019) and Fernando *et al.* (2021).

The compound construction of chitin tests was additionally described by Fourier transform infrared (FT-IR) spectroscopy utilizing FT-IR JASCO 4100 at Microanalytical Center, Fac. of Science, Cairo Univ. The specimens were contrasted with a straightforward KBr pellet at wavenumbers somewhere in the range of 400 and 400 cm^{-1} . The accompanying equation was utilized to work out the level of deacetylation (DDA) from FT-IR information as substantive by Baxter *et al.* (1992); Roy *et al.* (2017) and Taher *et al.* (2019):

$$DDA(\%) = 100 - \left[\frac{A_{1655}}{(A_{3450}) \times 115} \right]$$

where; A_{1655} and A_{3450} were absorbances at 1655 and 3450 cm^{-1} , respectively.

Preparation, Purification, and Characterization of Chitosan:

Chitosan powder was ready by deacetylation (DA) of chitin compounds CH1, CH2 and CH3 in 70% NaOH at $100 \text{ }^\circ\text{C}$ under a magnetic stirring for 36, 48 and 60 hrs, separately. The different time intervals were coded as Cs1, Cs2 and Cs3, individually. Chitosan compositions were courteous by solubilizing them in 0.5 M acidic arrangement, sifting them through paper, and afterward neutralizing them with 10% (w/w) NaOH up to pH 8. The precipitate was isolated and progressively washed with water and 70/30 V/V ethanol/water blends. The cleaned chitosan was at last dried at room temperature (Taher *et*

al., 2019). Chitosan samples were delineated by the solvency test according to Taher *et al.* (2019). As per the hour of deacetylation from the low time to the high, the compound design and the degree of N-deacetylation (DDA) of the chitosan distinguish by Fourier transform infrared (FT-IR) spectroscopy utilizing a similar strategy previously depicted. The Zeta potential of chitosan was assessed as a suspension in water. Estimations were performed utilizing a Malvern zetasizer 2000 at 37°C at Egyptian Petroleum Research Institute (EPRI), Nasr City. The zeta potential describes the contrast between the scattering medium attached to the scattered molecules and the transport medium attached to the transport medium (Taher *et al.*, 2019). Through electrostatic repulsion in between particles, this surface charge can significantly impact atom consistency quality in suspension (Taher *et al.*, 2019).

Preparation and Characterization of Chitosan Nanoparticles:

At the Egyptian Petroleum Research Institute (EPRI), Nasr City, RETSCH Planetary Ball Mills Type PM 400 was used to physically prepare chitosan nanoparticles. Chitosan powder (Cs1, Cs2 and Cs3) was charged and dry blended into 250 ml treated steel agar with 8 crushing balls at 3400 rpm for 6 hrs and afterward, for 12 hrs, to concentrate on the impact of ball-processing time. After the transformation of chitosan to the nanosize for 6 hrs, the code name of Cs1, Cs2 and Cs3 samples were changed to cs-nps1, cs-nps2 and cs-nps3, separately and for 12 hrs, the code name was likewise, changed to Cs-NPs1, Cs-NPs2 and Cs-NPs3, individually. Chitosan nanoparticles after 6 and 12 hrs ball-processing were described utilizing the dissolvability test as recently referenced. To investigate the particle size of chitosan nanoparticles: cs-nps1, cs-nps2, cs-nps3, Cs-NPs1, Cs-NPs2 and Cs-NPs3 (6 and 12 hrs), they were suspended, separately in water and sonicated for 3 min to obtain a homogenous suspension. A drop of the diluted suspension was saved onto shine released carbon-covered microscopy matrix, stained with a 1% phosphotungstic acid arrangement. samples were air-dried at room temperature and analyzed by transmission electron microscopy utilizing Philips 400 TEM, at 80 kV at The Regional Center for Mycology and Biotechnology, Al-Azhar Univ. (Taher *et al.*, 2019). On one hand, the degree of N-deacetylation (DDA) was carried out at Microanalytical Center, Fac. of Sci., Cairo Univ. On the other hand, the particle size distribution, polydispersity index (PDI), and zeta potential of chitosan nanoparticles were investigated in colloidal suspension using Zetasizer 2000 (Malvern Instrument Co., UK) at Egyptian Petroleum Research Institute (EPRI). Prior to the examination, chitosan nanoparticles were ultrasonically scattered in refined water for one min. The sample was analyzed by a horizontal angle X-ray beam. Dissipating radiates reflected from the sample showed the molecule size and circulation of the sample (Taher *et al.*, 2019). The molecule size conveyance was accounted for as a PDI esteem, which went from 0.0 to 1.0. Esteems near zero showed a homogeneous scattering, and those more noteworthy than 0.5 demonstrated a high heterogeneity (Dadras *et al.*, 2013).

Collection and Characterization of Scorpion Venom:

Leiurus quinquestriatus were kept alive in discrete plastic holders at the Lab, fed with cockroaches and mealworms, and got water as needed. The crude venom was gathered utilizing the electrical excitement (12-16 Volt) of the scorpion telson as per the technique made by Abdel-Rahman, Quintero-Hernandez and Possani (2013) and (Salem *et al.* (2016). For drying and sanitization, gathered the pooled venom was soluted in refined water and centrifuged at 5000 rpm for 10 min, to eliminate the cell flotsam and jetsam. At the earliest opportunity, the supernatant was shipped to Vacsera, Dokki to freeze-dried utilizing Genway Freeze Dry Framework to purge and convert to powder. The subsequent powder was coded as V and put away at -20 °C until utilized. The venom was likewise

characterized through just FT-IR spectroscopy, utilizing a similar technique recently referenced.

The experiments comply with the arrival guidelines and are carried out following the National Research Council's Guide for the care and use of laboratory animals.

Preparation and Characterization of Chitosan Nanoparticles Loading Venom:

Going to depend on Dadras *et al.* (2013) and Mohammadpour Dounighi *et al.* (2012), chitosan nanoparticles were prepared at National Research Center (NRC), Dokki by reacting sodium tripolyphosphate (STPP) anions with samples of chitosan Cs1, Cs2 and Cs3. The authors suggested that the optimal concentrations used were chitosan 2 mg/mL, 500 µg/mL venom, 1 mg/mL TPP, and chitosan /TPP ratio 2:1. The current samples of venom-loaded chitosan nanoparticles were coded V-CN1, V-CN2 and VCN3, respectively. Encapsulation efficiency (EE) of scorpion venom (V) and loading capacity (LC) of chitosan was assessed by evaluation of free poisons in the supernatant after centrifugation of samples at 20.000 rpm at +4°C for 30 min as per the following equations ('Bradford, 1976; Rashidi *et al.*, 2016; Khan, Saeed and Khan, 2019):

$$EE \% = \left(\frac{\text{Total amount of venom} - \text{Free amount of venom}}{\text{Total amount of venom}} \right) \times 100$$

$$LC \% = \left(\frac{\text{Total amount of venom} - \text{Free amount of venom}}{\text{Nanoparticles weight}} \right) \times 100$$

V-CN1, V-CN2, and V-CN3 samples were additionally distinguished through similar strategies as previously mentioned: FT-IR spectroscopy, dynamic light dissipating (DLS), transmission electron microscopy (TEM), polydispersity file (PDI) and zeta potential.

Statistical Analysis:

Statistical Package for Social Science (SPSS) version 25.0 statistical software was used to statistically analyze the data. The mean and standard deviation (S.D.) of the values were displayed. One-way ANOVA was used to compare the statistical differences between the groups, and the mean difference was significant at the P b 0.05 level.

RESULTS AND DISCUSSION

Extraction and Characterization of Chitin:

In the ongoing study, five grams of dried exoskeleton powder from every scorpion were utilized to extract chitin (Fig. 1). These powders were found to contain 19.7 %, 15.4 % and 15 % chitin, respectively (Table 1). The mean substance of chitin in the exoskeleton and tail powder of *L. quinquestriatus* scorpion was significantly higher than that in the two others. Kaya, Asan-Ozusaglam and Erdogan (2016) found the percentage of chitin in the exoskeleton of another scorpion species *Mesobuthus gibbosu* was only 12.4%. In the current study, notwithstanding the presence of chitin in the exoskeleton powder of scorpions, proteins, minerals, and colors were found, as well (Table 1). Chitin samples were characterized utilizing the solvency test which was organized in Table 2. The ongoing outcomes resembled the outcomes previously reported (Baxter *et al.*, 1992; Jayakumar *et al.*, 2010; Roy *et al.*, 2017; Ou *et al.*, 2018).

FT-IR information was utilized to decide the underlying structure of the current chitin samples and DDA. FT-IR showed the vanishing of absorption bands at 1540 cm⁻¹, demonstrating the fruitful deproteinization of the extracted chitin (Fig. 2a and Table 4). These outcomes were that way acquired by Taher *et al.* (2019).

In the present chitin spectra, the two bands at 1659 cm⁻¹ and 1624 cm⁻¹ related to the extending of amide I, and the bands at 1659 cm⁻¹ was relegated to the stretching of the

C-O bunch hydrogen clung to N-H of the adjoining intra-sheet chain, the 1624 cm^{-1} bands might show a particular hydrogen obligation of C-O with the hydroxyl-methyl gathering of the following chitin buildup of a similar chain, absorption bands at 1556 cm^{-1} related to amide II (N-H bending), the vanishing of ingestion groups at 1595 cm^{-1} demonstrated NH₂ absence of absorption bands at 1315 cm^{-1} confirmed to amide III (C-N extending). The results of the aftereffects of the ongoing examination matching to the consequences of Dahmane *et al.* (2014).

Table 1: Components of the three scorpions' exoskeleton and tail powder

Species	<i>Leiurus quinquestratus</i>		<i>Androctonus crassicauda</i>		<i>Androctonus amoreuxi</i>	
	Weight (g)	Percent (%)	Weight (g)	Percent (%)	Weight (g)	Percent (%)
Proteins	$2.26 \pm 0.14^*$	45.20	2.51 ± 0.04	50.20	2.56 ± 0.02	51.2
Minerals	$1.43 \pm 0.03^*$	28.60	1.35 ± 0.02	27.00	1.30 ± 0.03	26.0
Pigments	0.33 ± 0.02	6.50	0.37 ± 0.04	07.40	0.39 ± 0.03	07.8
Chitin	$0.98 \pm 0.13^*$	19.70	0.77 ± 0.02	15.40	0.75 ± 0.03	15.0

* Means at the same raw were significant compared with the other species.

Table 2: Chitin solubility test.

Solution	LiCl	H ₂ SO ₄	HCL	A mixture of H ₂ SO ₄ and HCL
	Solubility time (min)			
CH1	9.4	16.1	20.6	14.3
CH2	9.6	16.6	20.2	14.6
CH3	9.6	16.4	20.4	14.5

The steep assimilation peak at 1655 cm^{-1} was assigned to the ketone C-O in the current investigation, and the band's district at 2918 cm^{-1} showed that the C-H alkane vibration was impacted by the linkage of chitin solid force. The alkane bending vibration of C-H bunches with varying force was also present at the beak at 1379 cm^{-1} . While the cluster of groups between 450 cm^{-1} and 1750 cm^{-1} was typical for the amidic group (the bands "amide I" and "amide VI"), the peak at 1073 cm^{-1} confirmed the presence of C-O stretching of alcohol. This wide range of results matched with Srinivasan, Kanayairam and Ravichandran, (2018) 's findings.

The wide peak around $3600 - 3200\text{ cm}^{-1}$ in the present flawless chitin ought to be allocated to the extending vibration of - OH as affirmed by Mohammadpour Dounighi *et al.* (2012) and Mirzaei *et al.* (2017). However, Hajji *et al.* (2014) proposed that strong and well-defined bands at 1436 cm^{-1} (CH₂) were displayed in β chitin range, which was not found in any spectrum of the current chitin samples.

Also, Jang *et al.* (2004) proposed that in the FT-IR spectra of β -chitin, new bands were uncovered at 1603 cm^{-1} and 1650 cm^{-1} , which were not tracked down in the current work. While bands at 1429 cm^{-1} happened in the spectra of the current chitin samples, and this affirmed that it belonged to α chitin (Hajji *et al.*, 2014). Also, Kellersztein *et al.* (2019) believed that the protein architecture of the scorpion chela cuticle contained fibres of α -chitin.

DDA of the current chitin samples of the scorpions LQ, AC and AA were 10.90 %, 12.83 % and 11.30 %, respectively. Kaya, Asan-Ozusaglam and Erdogan (2016) produced chitin from *Mesobuthus gibbosus* scorpion and the DDA of chitin was 9.3 %.

The presence of amino groups in this extracted chitin before the DA process happened during the deproteinization step resembled the outcomes got by Maeda and Kimura (2004), Muzzarelli, (2012) and Küçükgülmez, (2018).

Chitosan Preparation and Characterization:

As indicated by deacetylation time, the yield of the current chitosan was 48.00 - 68.02 % after the preparation and purification. This decrease in the weight of chitin tests after deacetylation may be brought about by the replacement of acetyl bunches with amino ones (Muzzarelli, 2012). According to Kaya, Asan-Ozusaglam and Erdogan (2016), the *Mesobuthus gibbosus* scorpion's chitin content and chitosan output were found to be 12.4% and 78.4%, respectively. As displayed in Table 3 in this examination, the percentage of chitosan yield was inversely proportional to the deacetylation time, which concurred with the outcomes recorded by Muzzarelli (2012). The duration of the current chitosan's solubility in acetic acid was also, inversely proportional to the deacetylation time (Table 4), like the results previously obtained by Ravi Kumar (2000), Zhang *et al.* (2012) and Taher *et al.* (2019). This may be because chitosan had a larger concentration of protonated free amino groups, which attract ionic mixes and allow chitosan to degrade more quickly in acidic solutions (Taher *et al.*, 2019). The current chitosan samples had a pale yellow to yellow color, which was approximately the same result obtained by Taher *et al.* (2019). These chitosan nanoparticles were analyzed by FT-IR spectroscopy, the spectra were represented in Fig. 2b and Table 4, and all distinguishing peaks for the chitosan useful gatherings were noticeable.

Table 3: Production and solubility of the present chitosan according to DA time

Chitin (g) *	Chitosan sample	DA time (hrs)	Yielded chitosan before purification		Yielded chitosan After purification	
			(g)	(%)	(g)	(%)
2.95 (CH1)	Cs1	36	2.11	71.40	2.01	68.02
2.31 (CH2)	Cs2	48	1.60	69.26	1.31	56.70
2.25 (CH3)	Cs3	60	1.20	53.33	1.08	48.00

The total amount of product chitin in 3 trials in each scorpion species.

The vanishing of assimilation bands at 1540 cm^{-1} indicated that the current chitosan samples had efficient deproteinization. Too, the absorption bands used to recognize minerals (1798 and 876 cm^{-1}) vanished. The sharp extreme assimilation bands at 1655 cm^{-1} were the trademark peak for prime amino groups (NH_2) of chitosan (from which DDA was determined). This result was that way recently announced by Taher *et al.* (2019) and Lazaridou *et al.* (2020).

As shown in Fig. 2b, the bands at 3450 cm^{-1} were suitable for the hydroxyl groups (OH) of chitosan and might be actual adsorbed water particles, which agreed with the findings recently observed (Taher *et al.*, 2019). Furthermore, the disappearance of the absorption bands at 1556 cm^{-1} corresponded to the disappearance of amide II (N-H bending). The new apex at 1595 cm^{-1} is compatible with NH_2 twisting. The bands with the most extreme absorption showed up at 2870 cm^{-1} , attributable to the valence's vibrations of the bending C-H and the wide apex around $3600 - 3200\text{ cm}^{-1}$ in neat chitosan ought to be doled out to the extending vibration of - OH, which resembled the consequences of Dahmane *et al.* (2014) and Lazaridou *et al.* (2020). The assimilation bands at 2921 and 2877 cm^{-1} can be ascribed to C-H symmetric and uneven extending, respectively. Fruitful deacetylation of the current chitin to switch over completely to chitosan was perceived by NH_2 functional groups are increased (708 cm^{-1} , 1655 cm^{-1} , and 3111 cm^{-1}) and diminishing C-O main set (1661.7 cm^{-1}), and it resembled the

outcomes acquired by Taher *et al.* (2019) and Antonino *et al.* (2017). The occurrence of bands at 1423 and 1375 cm^{-1} , respectively, confirmed the CH₂ bending and CH₃ symmetrical deformations (Antonino *et al.*, 2017). While regularity extending of C-O-C was observed around 1070 cm^{-1} . Because of the presence of saccharides in the chitosan structure, the peak at 570 cm^{-1} developed, correlating with the findings reported by Mirzaei *et al.* (2017). DDA values were determined and tabulated using the intensity of the assimilation groups at 1655 cm^{-1} and 3450 cm^{-1} , respectively, using the previously cited Baxter's equation (Baxter *et al.*, 1992) (Table 4). Kaya, Asan-Ozusaglam and Erdogan (2016) claimed that a 70.5% DDA of scorpion chitosan with 50% NaOH at 150°C and 500 rpm for 4 hrs was discovered. Malvern zetasizer was utilized to assess the zeta potential of the chitosan specimens (Cs1, Cs2, and Cs3) and the outcomes are displayed in Fig. 5a-c and Table 5. The high positive charges (high amino groups) were shown by the zeta potential and the steadiness against accumulation for charged balanced system (Zhang *et al.*, 2012). zeta potential showed a positive charge for all the current chitosan samples, and it was straightforwardly relative to DDA due to the increase of the amino groups (Table 5).

Nano-size of Chitosan Preparation and Characterization:

One of the primary reasons for using scorpion chitosan nanoparticles in the current experiment was the conclusion that they have high action against microbes (seven bacterial species and two yeast species) (Kaya, Asan-Ozusaglam and Erdogan, 2016). Chitosan nanoparticles also have a long shelf life (Zhao *et al.*, 2018). Additionally, it has been found that the nano-size of chitosan has strong protein interaction capabilities (Zhao *et al.*, 2018).

The ball-milling method was used in the current study to physically create chitosan nanoparticles. The hue of the current chitosan nanoparticles changed from light gray after 6 hrs to gray after 12 hrs of ball-milling. All samples of the current chitosan nanoparticles were dissolved in 1.0 % acetic acid more easily than the chitosan samples, and with an inversely proportional to both the deacetylation time and particle size (Table 4). Chitosan nanoparticles were analyzed using FT-IR spectroscopy to determine the chemical structure, and calculate DDA from data of spectra, the results were shown in Figures. 2c, d and Table 4, illustrating that the peaks of chitosan nanoparticles (6- and 12-hrs ball-milling) were approximately the same in the present chitosan samples (Cs1, Cs2 and Cs3). These results confirmed that the ball-milling can be used to decrease the size of the particle, without any change to the functional group properties. However, a slight difference in the DA degree was observed. This might be caused by very little crystallization damage in chitosan (Taher *et al.*, 2019),(Sari *et al.*, 2019). Additionally, Laka and Chernyavskaya (2006) concluded that following ball-milling, the DDA of the produced chitosan nanoparticles did not vary appreciably. Figures. 3a-f and 4a-f and Table 4 in this study showed that the intensity and number-weighted distribution achieved by DLS for chitosan nanoparticles revealed that 100% of these samples had a homogenous particle size less than 250 nm after 6-hrs ball-milling and less than 100 nm after 12-hrs ball-milling. Moreover, a somewhat constrained and homogeneous size dispersion of the current chitosan nanoparticles was visible in the histogram of their number-weight distribution (Figs. 4a-f). The DLS measurements of the chitosan nanoparticles in Table 4 demonstrated that they were not just extremely well monodispersed but also exhibited great suspension quality (Taher *et al.*, 2019),(Agarwal *et al.*, 2018). Additionally, the modern chitosan nanoparticles' PDI readings were less than 0.3, indicating that they may be dependably measured to be monodisperse (Taher *et al.*, 2019). The electrical charge of nanoparticles was determined by the zeta potential, which was the electric potential in the interfacial double layer of dispersed particles (Taher *et al.*, 2019), (Agarwal *et al.*, 2018).

Chitosan nanoparticles were investigated here, and their zeta potential was directly related to DDA and inversely proportional to particle size. (Table 4 and Figs. 5d-i). These zeta potential values can be used as a measure of the stability against the accumulation of charged stabilized systems and the high positive charges (high amino groups) (Soon *et al.*, 2018). After 6 hrs of ball-milling (Figs. 6a–c), TEM graphs of the present chitosan nanoparticles revealed uniform particles with a spherical shape that were smaller than 230 nm and less than 25 nm after 12 hrs of ball-milling. (Fig. 7a-c). Taher *et al.* (2019) discovered that the generated chitosan nanoparticles by ball-milling had a particle size smaller than 20 nm after 6 hrs. The size of the chitosan nanoparticles in this study as estimated by dynamic light scattering (DLS) was somewhat bigger than that discovered using transmission electron microscopy (TEM). This outcome was in line with Agarwal *et al.* (2018) researcher who went on to say that since DLS monitored the hydrodynamic diameter of the molecules or particles in solution, it was a good indicator of the apparent size of the dynamically hydrated/solvated particles (The radius of the hypothetical hard sphere that diffuses at the same rate as the particles measured with DLS is known as the hydrodynamic diameter). The consistency of the produced chitosan nanoparticles was validated by the agreement between their intensity- and number-size distributions (Agarwal *et al.*, 2018).

Table 4: DDA of chitin, chitosan, and chitosan nanoparticles using FT-IR.

Sample	I ₁₆₅₅ ^a	I ₃₄₅₀ ^a	DDA (%) FT-IR	Color	Solubility time ^b (min)
CH1	84.71	80.72	10.90	Yellowish-brown	
CH2	91.99	89.57	12.83	Yellowish-brown	
CH3	89.17	86.19	11.30	Yellowish-brown	
Cs1	95.71	84.33	70.41	Pale yellow	7.50
Cs2	97.13	82.39	82.71	Yellow	4.50
Cs3	98.56	71.10	95.10	Yellow	2.50
cs-nps1	95.35	82.79	71.00	Light gray	5.00
cs-nps2	99.15	94.19	83.59	Pale gray	3.00
cs-nps3	98.89	74.98	95.54	Pale gray	1.50
Cs-NPs1	99.05	96.09	72.47	Gray	3.00
Cs-NPs2	98.71	90.99	84.18	Gray	2.10
Cs-NPs3	98.76	69.10	96.11	Gray	1.20

^a I₁₆₅₅ and I₃₄₅₀ were the light intensity of NH₂ and OH groups at 1655 and 3450 cm⁻¹, respectively.

^b Solubility in 1% acetic acid (v/v) solution without further heating or sonication.

Collection and Characterization of Scorpion's Venom:

In the present work, venom was only obtained from *Leiurus quinquestriatus* scorpion, because this species was easier to find and collect. It was collected using electrical stimulations. The current venom was initially a white fluid, which after purification and freeze-drying changed into a pale-yellow powder. Its description was done using FT-IR spectroscopy, and the absorption spectra showed that the peaks at 2118 cm⁻¹ and 2878 cm⁻¹ corresponded to the mean peaks of the venom. (Fig. 2e). These outcomes matched those attained by Dadras *et al.* (2013). On the one hand, the existence of an amino group of amino acids was said to be the cause of the distinctive bands at 3400-3300 cm⁻¹ in the current investigation. Then again, peaks at 1645 cm⁻¹ and 1540 cm⁻¹ coordinated with the discoveries of Dadras *et al.* (2013) and Asfour *et al.* (2021) and were associated with the peptide bonds' vibrations of C=O and C-N stretching, respectively. In this experiment, the band at 1415 cm⁻¹ indicated the twisting states of CH₂/CH₃ units in amino-acid side chains. In agreement with the findings of Rebbouh, Martin-Eauclaire and

Laraba-Djebari (2020), peaks around 1112 cm^{-1} and 1040 cm^{-1} revealed an unsystematic coil structure.

Development and Evaluation of *Leiurus quinquestriatus* Venom-Loaded Chitosan Nanoparticles:

In this study, venom-loaded chitosan nanoparticles (V-CN1, V-CN2, and V-CN3) had loading capacities (LC) of 72.60%, 73.20%, and 76.50%, respectively, and encapsulation efficiencies (EE) of 86.87%, 86.94%, and 87.98%, respectively. Mirzaei *et al.* (2017) suggested that prepared chitosan nanoparticles for loading *Echis carinatus* snake venom had an encapsulation efficiency (EE) and loading capacity (LC) of 94% and 87%, respectively. The protein molecules were completely confined inside the polymeric matrix of chitosan nanoparticles when the venom was absorbed in TPP liquid and cross-linked nanoparticles were produced, which explains this EE (Gan and Wang, 2007). Additionally, proteins were adsorbed on the surface of nanoparticles because of electrostatic interactions involving positively charged chitosan groups and negatively charged protein molecules (venom) during the formation of nanoparticles (Gan *et al.*, 2005). Peaks at 1645 cm^{-1} and 1540 cm^{-1} , respectively, which were the vibrational frequencies of the peptide bonds: C=O and C-N stretching as well as N-H bending modes, were visible in the FT-IR spectra of the venom-loaded chitosan nanoparticles (V-CN1, V-CN2, and V-CN3). The bands at 1415 cm^{-1} focused on how CH₂/CH₃ bunches bend in the side chains of peptide amino acids (Mirzaei *et al.*, 2017), (Rebbouh, Martin-Eauclaire and Laraba-Djebari, 2020), (Firouzeh *et al.*, 2021). The P=O group was shown by the bands at 1170 cm^{-1} , which also revealed the chemical interactions and confirmed the venom's effective loading within the polymeric chitosan nanoparticles (Mirzaei *et al.*, 2017), (Rebbouh, Martin-Eauclaire and Laraba-Djebari, 2020), (Firouzeh *et al.*, 2021) The hydrogen bonding between TPP and chitosan nanoparticles, which led to a considerably larger peak at this position, was also demonstrated by the peak at 3400 cm^{-1} , which was present (Mirzaei *et al.*, 2017). The apexes at 2118 cm^{-1} and 2878 cm^{-1} demonstrated the presence of venom in nanoparticles (Dadras *et al.*, 2013). Maybe because of the cross-connecting between the nanoparticles of chitosan and the scorpion venom, the peak at 1658 cm^{-1} was found (Mirzaei *et al.*, 2017). According to the most recent results obtained by DLS and in agreement with those obtained by Mohammadpour Dounighi *et al.* (2012), the diameters of chitosan nanoparticles that were loaded with venom were greater than those of chitosan nanoparticles alone (Figs. 3g - i and 4g - i) (Table 5). Because of the venom protein molecules' huge molecular weight and enormous size, these authors claimed that these results were plausible. Chitosan nanoparticles loaded with venom had PDI values of 0.426, 0.398, and 0.415, respectively, displaying a small and beneficial particles size distribution (PDI < 0.5) (Table 5) (Mohammadpour Dounighi *et al.*, 2012). The morphological properties and surface appearance of chitosan nanoparticles loaded with venom were shown in the present TEM graphs. The generally spherical to irregular-shaped nanoparticles were between 200 and 300 nm in size (Fig. 8 a-i). The Zeta potential of venom-loaded chitosan nanoparticles can have a substantial impact on how stable they are in suspension through electrostatic attraction between the particles (Mohammadpour Dounighi *et al.*, 2012). The current findings showed that the venom-loaded chitosan nanoparticles had respective zeta potentials of 19.31, 20.22, and 23.31 mV for V-CN1, V-CN2, and V-CN3, respectively (Figs. 5j-1) (Table 5). These results showed that the zeta potential of venom-loaded chitosan nanoparticles was somewhat reduced throughout their formation. The regularity of the venom's interaction with long-chain chitosan molecules was thought to be irregular (Mohammadpour Dounighi *et al.*, 2012).

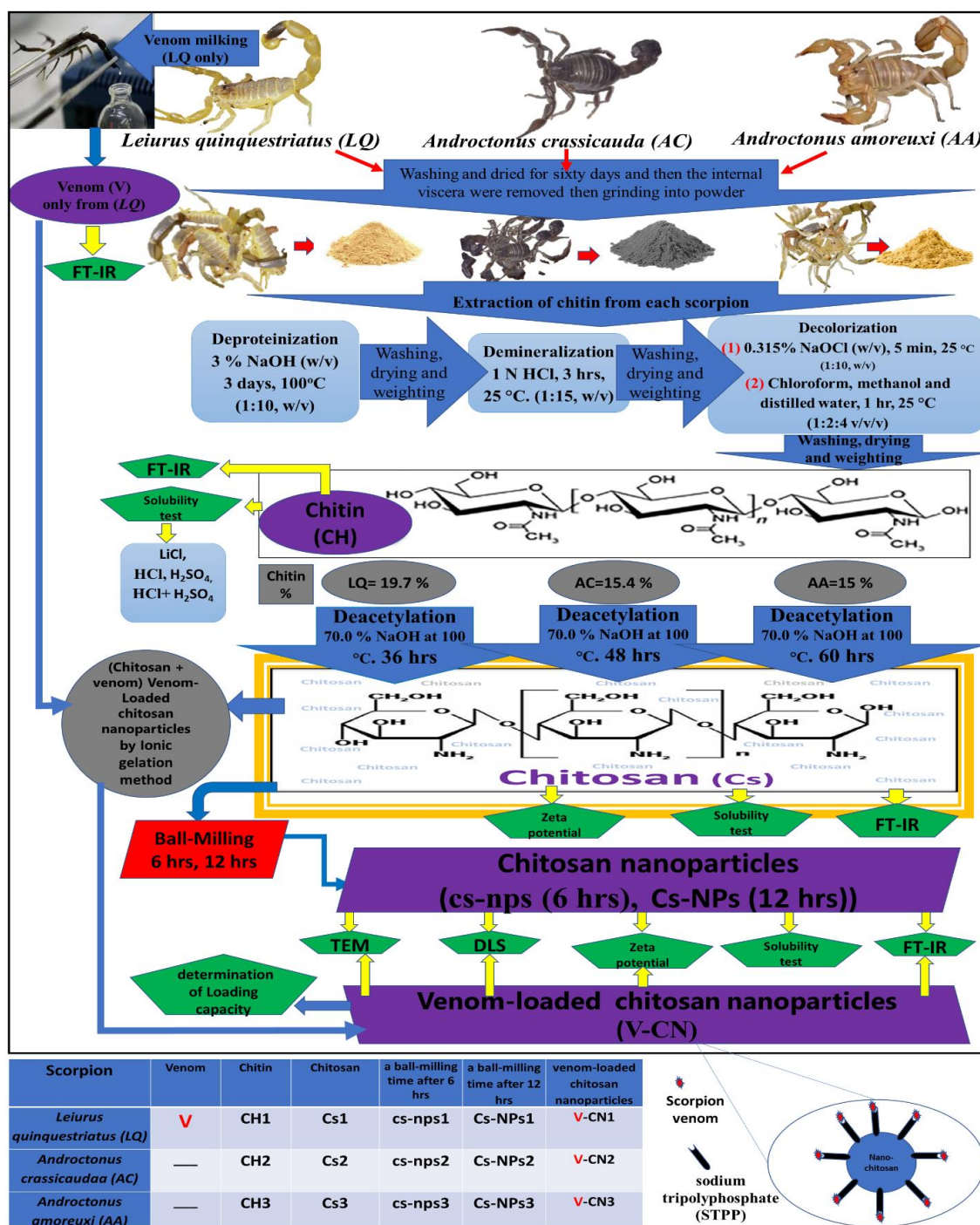


Fig. 1. Graphical abstract of preparation and characterization of chitin, chitosan and chitosan nanoparticles from three scorpion species *Leiurus quinquestriatus*, *Androctonus crassicauda*, and *Androctonus amoreuxi* and preparation of venom-loaded chitosan nanoparticles, blue arrows represented preparation steps and yellow arrows represented characterization.

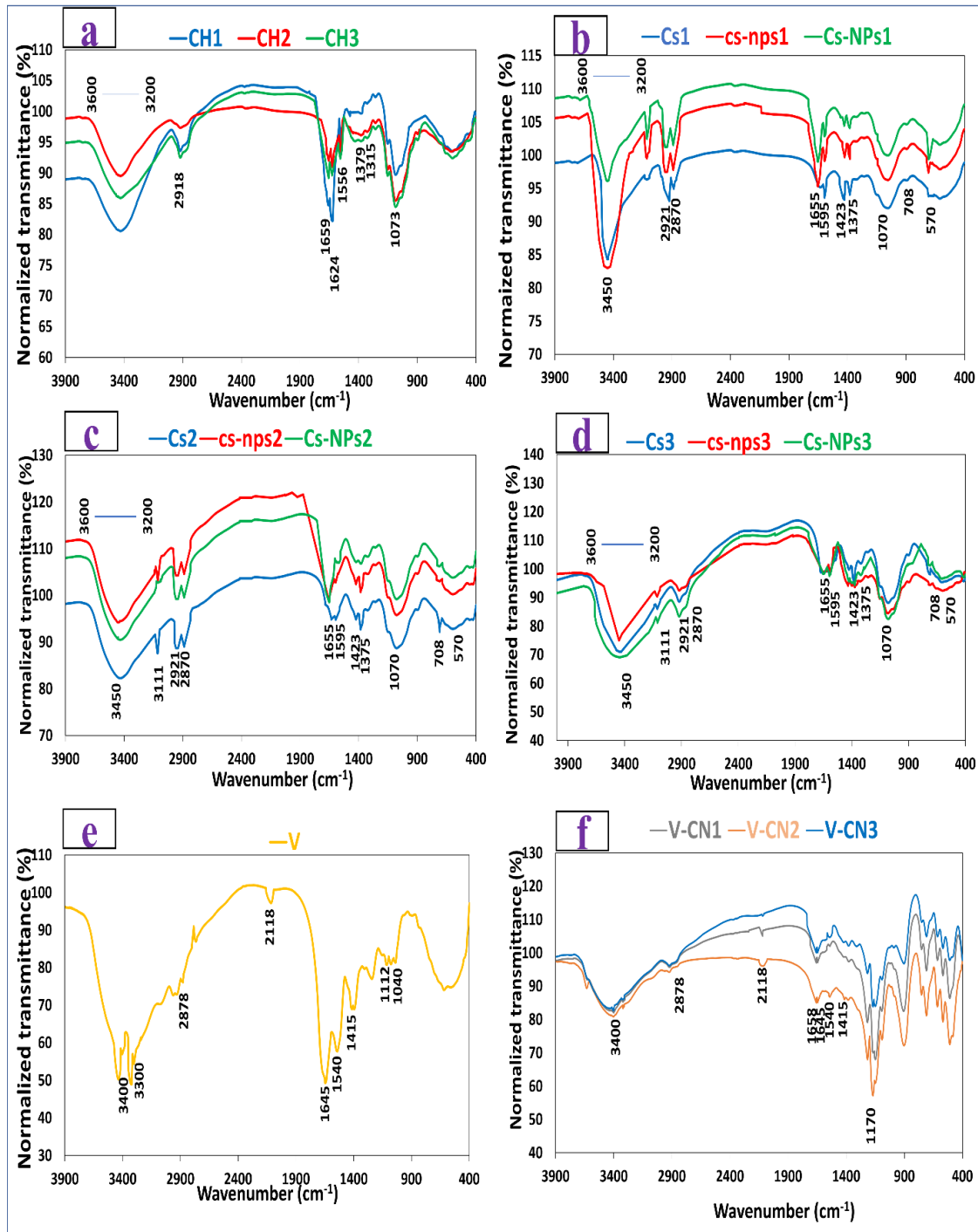


Fig. 2: Graphs representing the FT-IR spectra of (a) chitin (CH1, CH2, and CH3), (b-d) chitosan (Cs1, Cs2 and Cs3), chitosan nanoparticles after 6 hrs (cs-nps1, cs-nps2, and cs-nps3) and chitosan nanoparticles after 12 hrs (Cs-NPs1, Cs-NPs2, and Cs-NPs3), (e) venom (V) and (f) venom-loaded chitosan nanoparticles (V-CN1, V-CN2, and V-CN3).

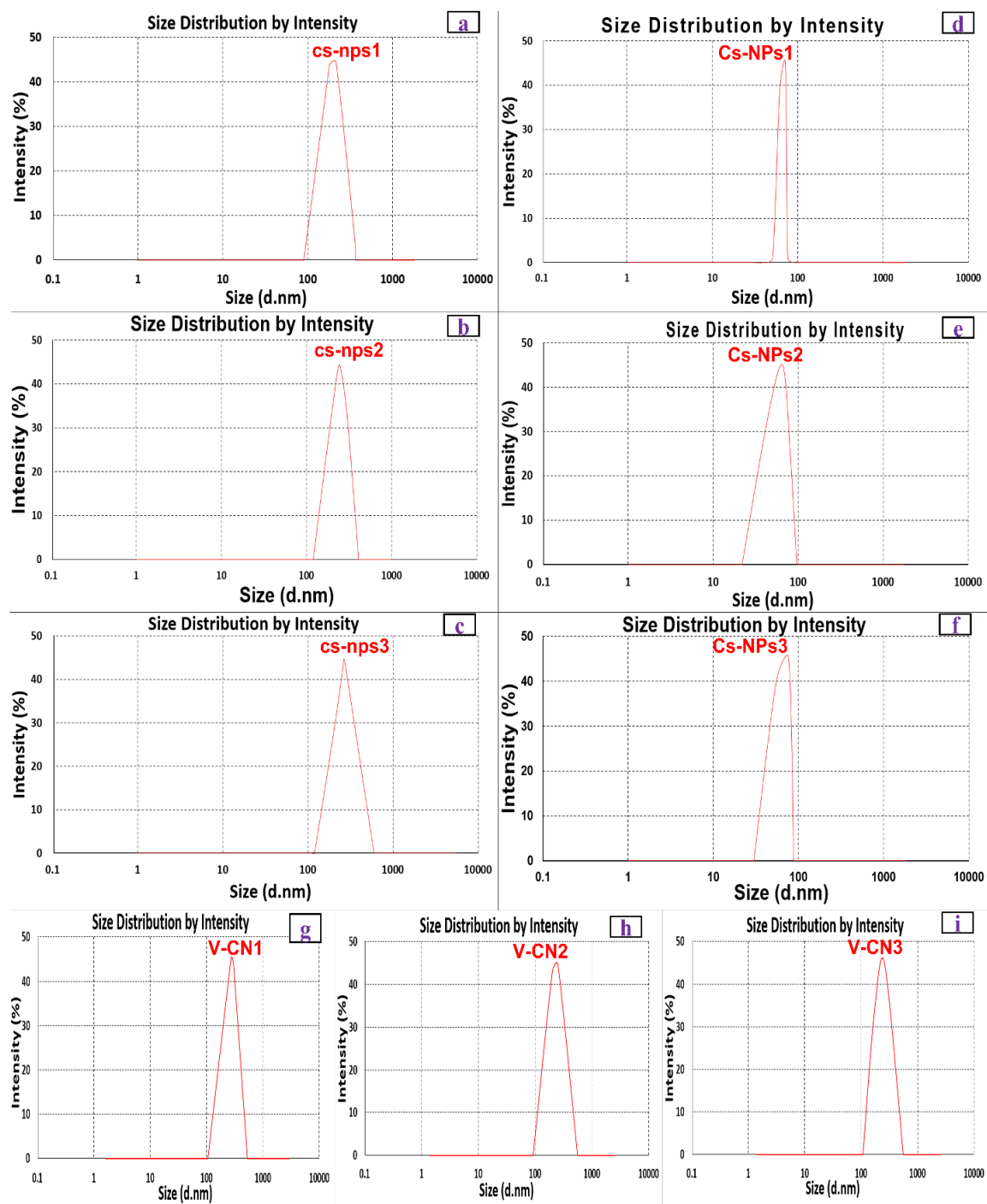


Fig. 3. Graphs showing the DLS of the current chitosan nanoparticles by the intensity – size distribution of chitosan nanoparticles after 6 hrs (a) cs-nps1, (b) cs-nps2 and (c) cs-nps3, chitosan nanoparticles after 12 hrs (d) Cs-NPs1, (e) Cs-NPs2 and (f) Cs-NPs3), and venom- loaded chitosan nanoparticles (g) V-CN1, (h) V-CN2 and (i) V-CN3.

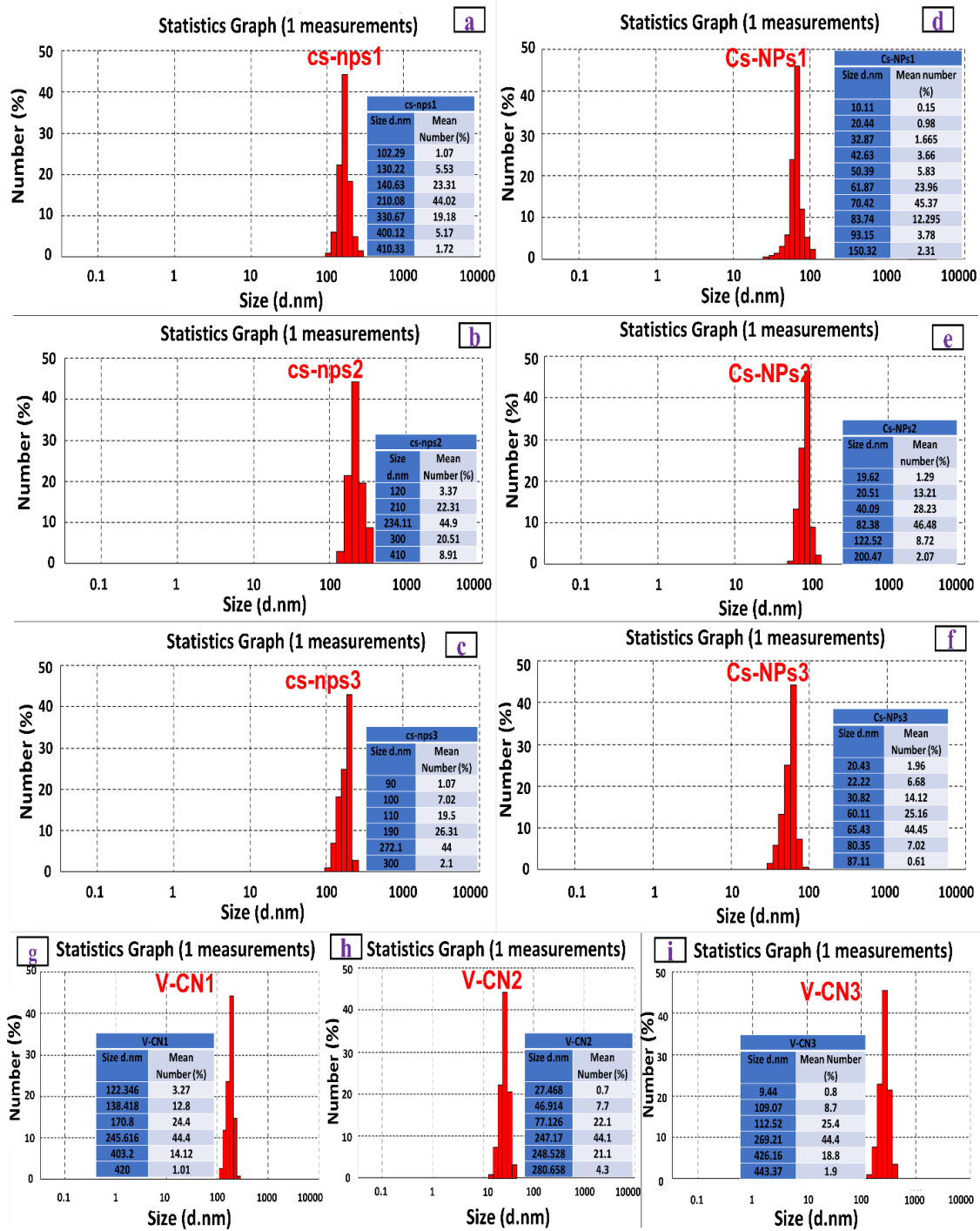


Fig. 4. Histogram of the number-weighted size distribution of chitosan nanoparticles after 6 hrs (a) cs-nps1, (b) cs-nps2 and (c) cs-nps3, chitosan nanoparticles after 12 hrs (d) Cs-NPs1, (e) Cs-NPs2 and (f) Cs-NPs3, and venom- loaded chitosan nanoparticles (g) V-CN1, (h) V-CN2 and (i) V-CN3.

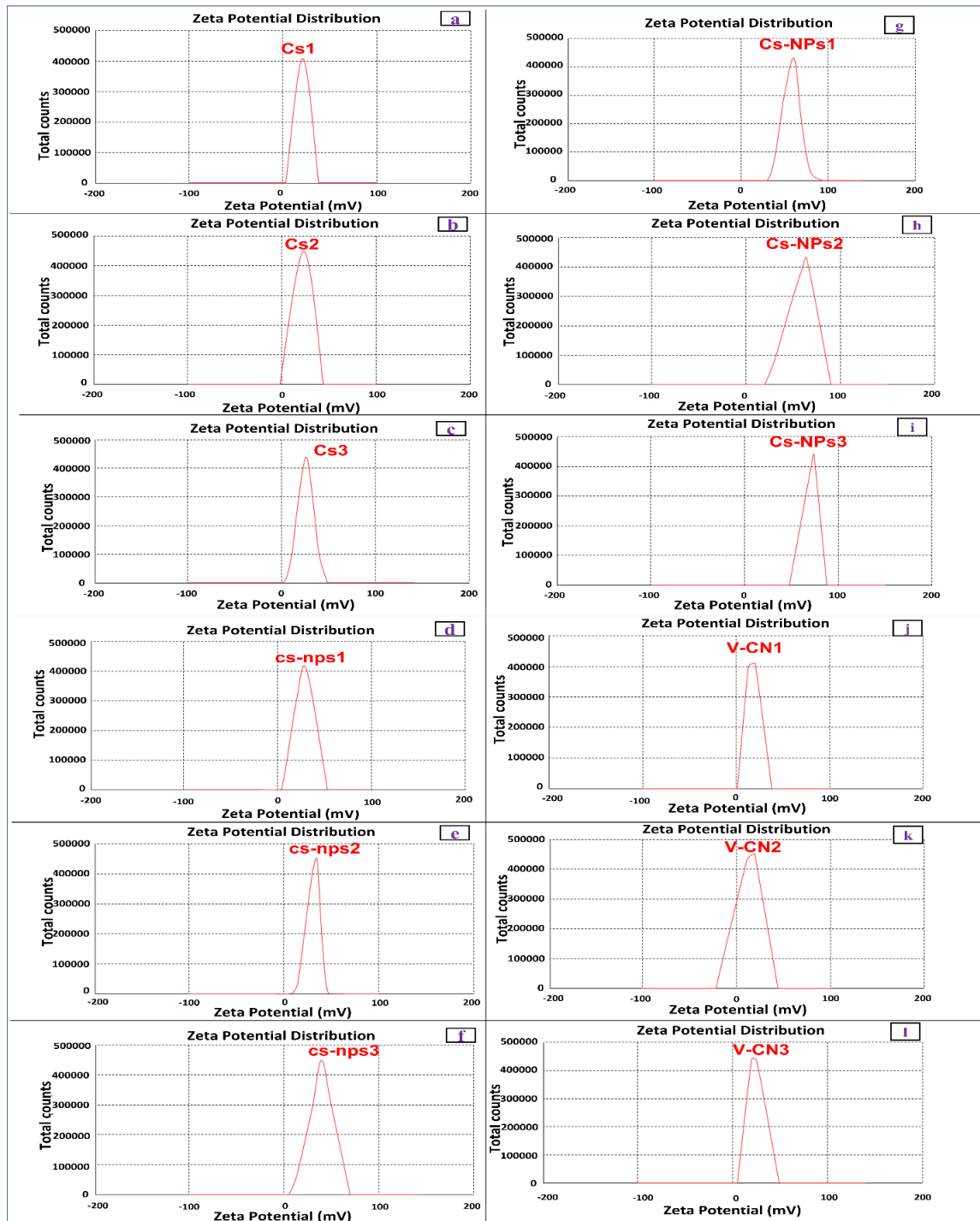


Fig. 5. Graphs showing zeta potential of chitosan (a) Cs1, (b) Cs2 and (c) Cs3, chitosan nanoparticles after 6 hrs (d) cs-nps1, (e) cs-nps2 and (f) cs-nps3, chitosan nanoparticles after 12 hrs (g) Cs-NPs1, (h) Cs-NPs2 and (i) Cs-NPs3), and venom- loaded chitosan nanoparticles (j) V-CN1, (k) V-CN2 and (l) V-CN3.

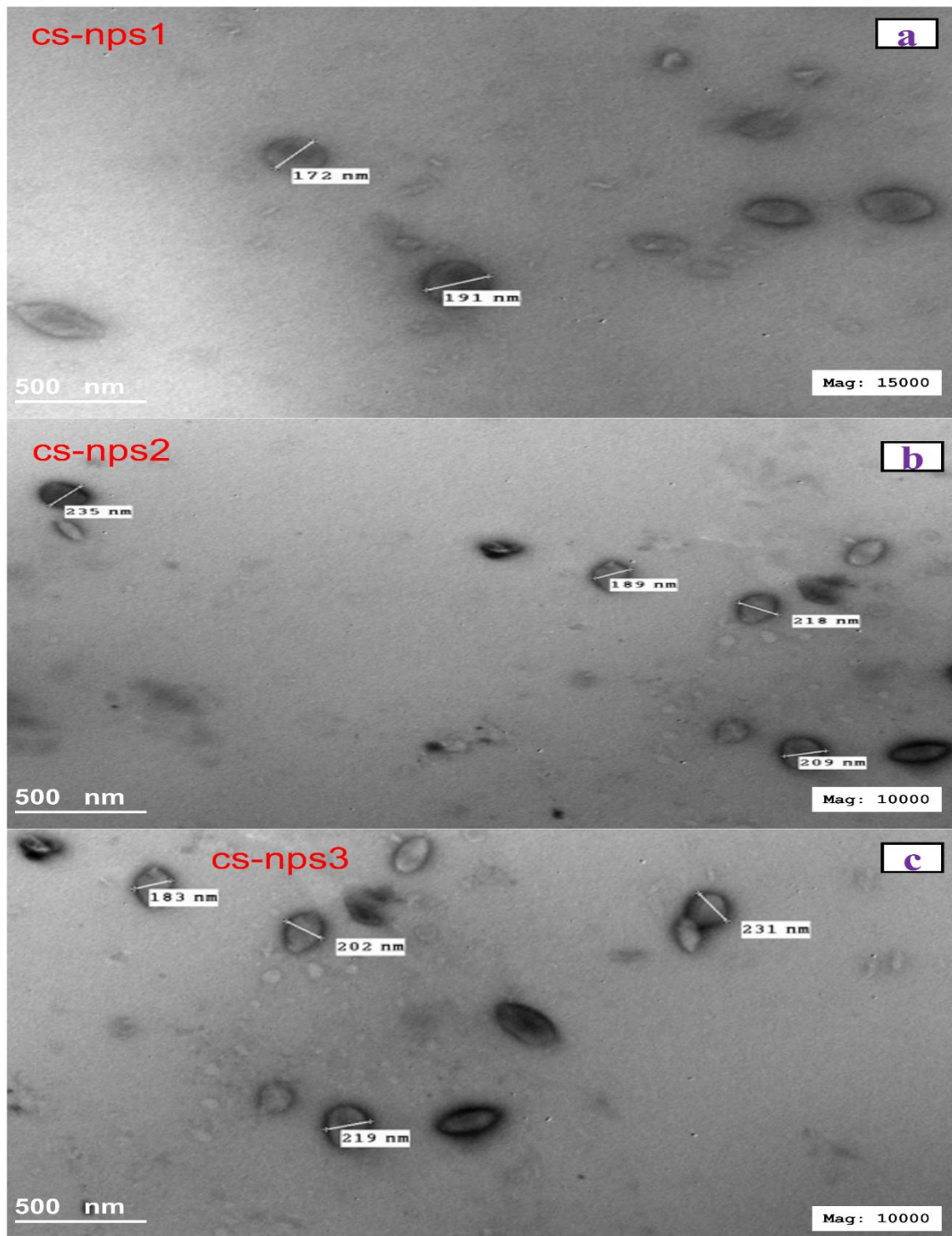


Fig. 6. TEM graphs of the chitosan nanoparticles after 6-hrs ball-milling (a) cs-nps1, (b) cs-nps2 and (c) cs-nps3.

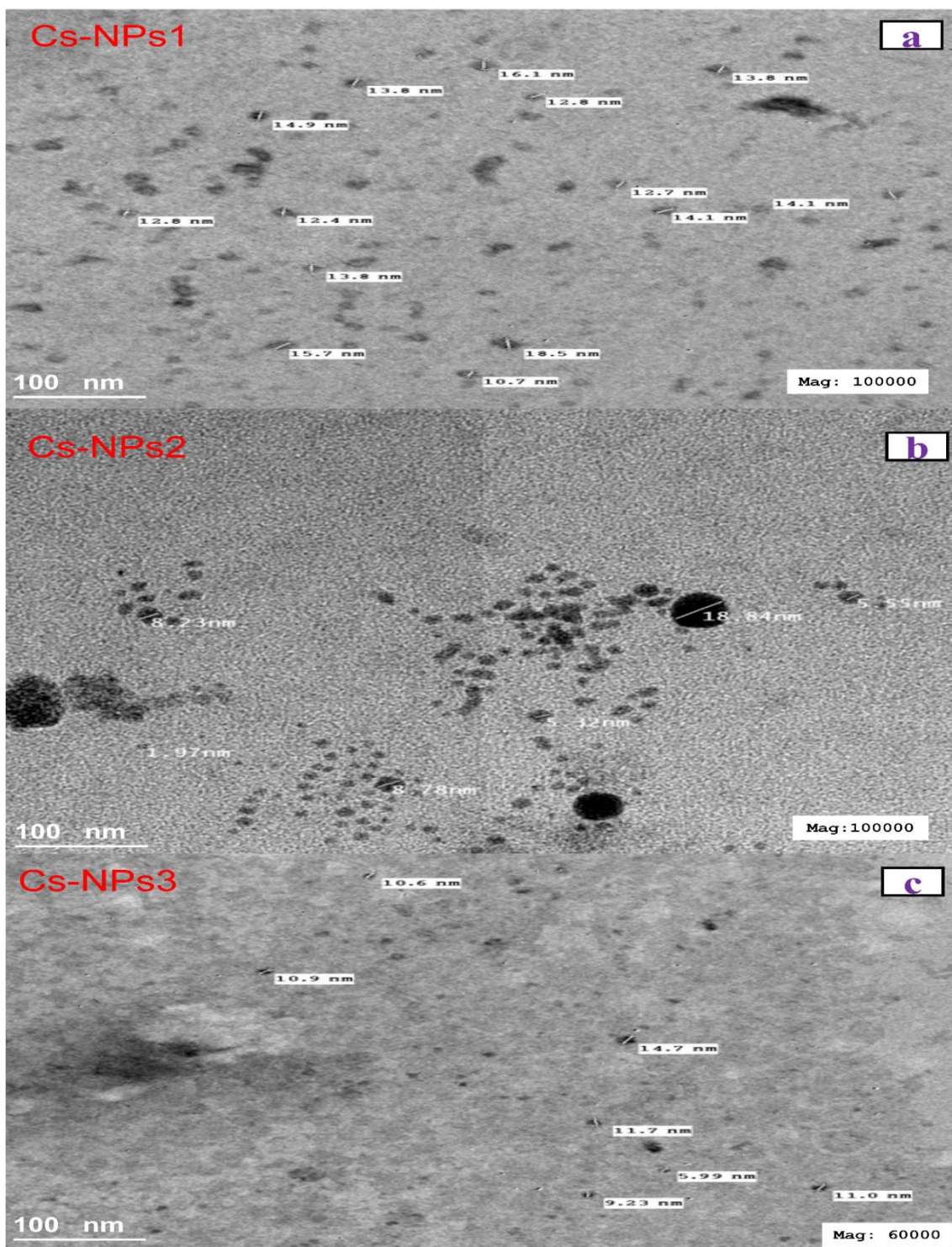


Fig. 7. TEM graphs of the chitosan nanoparticles after 12-hrs ball-milling (a) Cs-NPs1, (b) Cs-NPs2 and (c) Cs-NPs3.

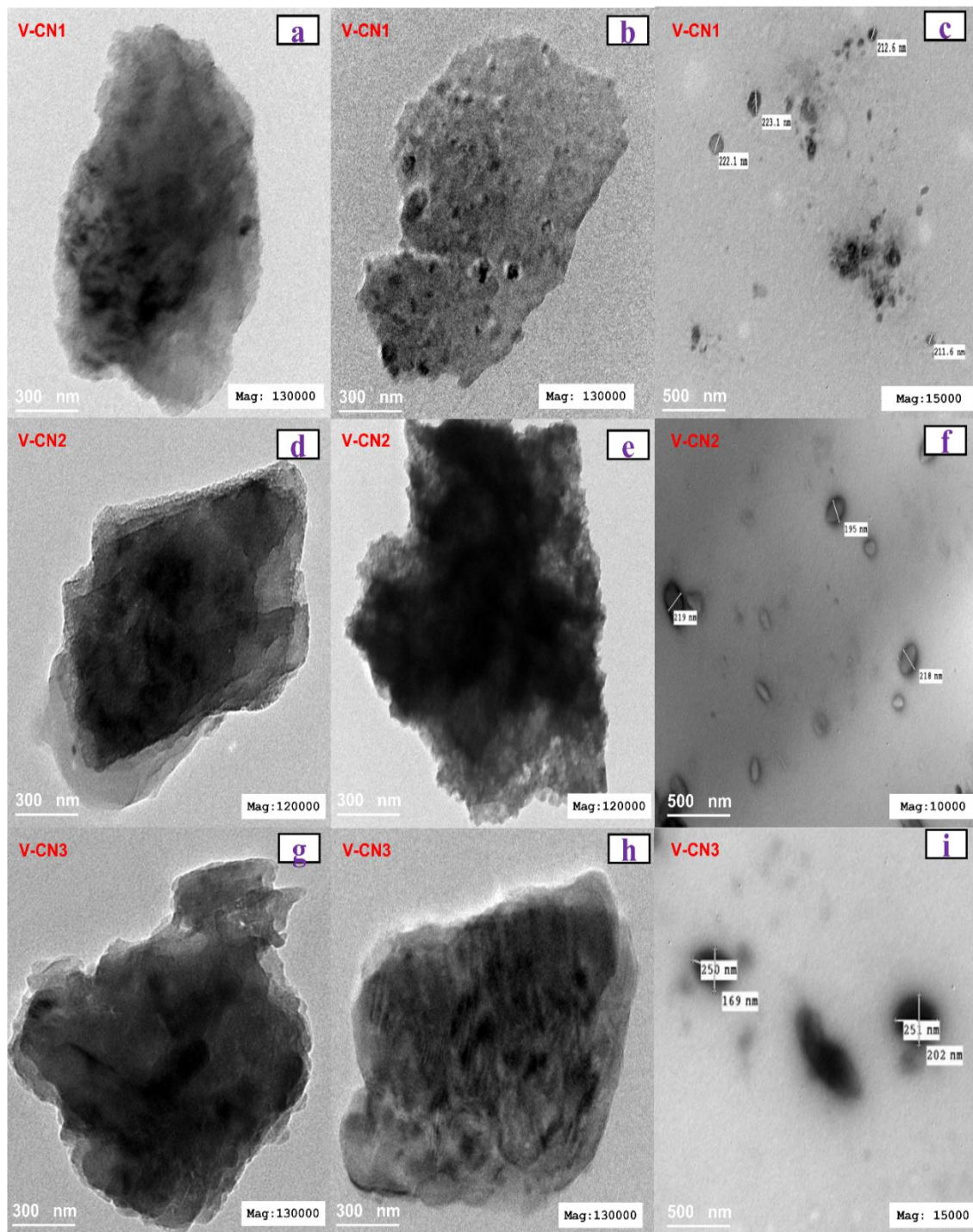


Fig. 8. TEM graphs of the scorpion venom-loaded chitosan nanoparticles (a,b) single nanoparticle of V-CN1, (c) nanoparticles of V-CN1, (d,e) single nanoparticle of V-CN2, (f) nanoparticles of V-CN2 and (g,h) single nanoparticle of V-CN3 and (i) nanoparticles of V-CN3.

Table 5: Particle size, PDI and zeta potential of chitosan and chitosan nanoparticles using a Malvern zetasizer

Sample	Size distribution by intensity (nm)	Size distribution by number (nm)	The polydispersity index (PDI)	Zeta potential (mV)
Cs1	—	-	-	21.16
Cs2	-	-	-	23.33
Cs3	-	-	-	26.11
cs-nps1	216.13	210.08	0.292	30.40
cs-nps2	244.59	234.11	0.278	35.45
cs-nps3	270.12	272.10	0.286	39.70
Cs-NPs1	72.32	70.42	0.288	60.24
Cs-NPs2	83.26	82.38	0.280	64.23
Cs-NPs3	77.18	65.43	0.286	74.21
V-CN1	280.88	245.61	0.426	20.16
V-CN2	252.91	247.17	0.398	19.33
V-CN3	259.19	269.21	0.315	24.59

Conclusion

This study is the first to prepare chitin, chitosan, chitosan nanoparticles, and chitosan nanoparticles with venom from three scorpions. The produced venom-loaded chitosan nanoparticles ranged in size from 200 to 300 nm, with a loading capacity of 72 to 76%, an encapsulation efficiency of 86 to 87%, and an acceptable PDI. These characteristics made the scorpion venom-loaded chitosan nanoparticles appropriate for a wide range of biological and pharmacological uses.

Funding Resources:

This research did not receive any specific grant from funding agencies in the public, commercial, or not-for-profit sectors.

Statements and Declarations:

No potential conflict of financial or non-financial interest was reported by the authors.

REFERENCES

- Abd El-Aziz, F.E.Z.A. *et al.* (2019): 'Toxicological and epidemiological studies of scorpion sting cases and morphological characterization of scorpions (*Leiurusquin questriatus* and *Androctonus crassicauda*) in Luxor, Egypt', *Toxicology Reports*, 6(March), pp. 329–335. Available at: <https://doi.org/10.1016/j.toxrep.2019.03.004>.
- Abdel-Rahman, M.A., Quintero-Hernandez, V. and Possani, L.D. (2013): 'Venom proteomic and venomous glands transcriptomic analysis of the Egyptian scorpion *Scorpio maurus palmatus* (Arachnida: Scorpionidae)', *Toxicon*, 74, pp. 193–207. Available at: <https://doi.org/10.1016/j.toxicon.2013.08.064>.
- Agarwal, M. *et al.* (2018): 'Preparation of Chitosan Nanoparticles and their In-vitro Characterization', *International Journal of Life-Sciences Scientific Research*, 4(2), pp. 1713–1720. Available at: <https://doi.org/10.21276/ijlssr.2018.4.2.17>.
- Ahmadi, S. *et al.* (2020): 'Scorpion venom: Detriments and benefits', *Biomedicines*, 8(5). Available at: <https://doi.org/10.3390/BIOMEDICINES8050118>.
- Akef, H.M. (2019): 'Anticancer and antimicrobial activities of scorpion venoms and their peptides', *Toxin Reviews*. 38 (1) 1-13. Available at: <https://doi.org/10.1080/15569543.2017.1414847>.

- Alqahtani, A.R. and Badry, A. (2021): 'A contribution to the scorpion fauna of Saudi Arabia, with an identification key (Arachnida: Scorpiones)', *Journal of King Saud University-Science*. 33 (4) 1-13. Available at: <https://doi.org/10.1016/j.jksus.2021.101396>.
- Antonino, R.S.C.M.D.Q. *et al.* (2017): 'Preparation and characterization of chitosan obtained from shells of shrimp (*Litopenaeus vannamei* Boone)', *Marine Drugs*, 15(5), pp. 1–12. Available at: <https://doi.org/10.3390/md15050141>.
- Asfour, H.Z. *et al.* (2021): 'Phyto-Phospholipid conjugated scorpion venom nanovesicles as promising carrier that improves efficacy of thymoquinone against adenocarcinoma human alveolar basal epithelial cells' *Pharmaceutics*. 13 (12) 1-19. <https://doi.org/10.3390/pharmaceutics13122144>.
- Attarde, S.S. and Pandit, S. v. (2016): 'Scorpion venom as therapeutic agent - current perspective', *International Journal of Current Pharmaceutical Review and Research*, 7(2), pp. 59–72.
- Baxter, A. *et al.* (1992): 'Improved method for I.R. determination of the degree of acetylation of chitosan', *International Journal of Biological Macromolecules*., 14, pp. 166–169.
- Bradford, M.M. (1976): A rapid and sensitive for the quantitation of microgram quantities of protein utilizing the principle of protein-dye binding. *Analytical Biochemistry*. 72, pp. 248-254. <https://doi.org/10.1006/abio.1976.9999>
- Coelho, P. *et al.* (2017): 'A "striking" relationship: scorpion defensive behaviour and its relation to morphology and performance', *Functional Ecology*, 31(7), pp. 1390–1404. Available at: <https://doi.org/10.1111/1365-2435.12855>.
- Dadras, O.G. *et al.* (2013): 'Preparation, characterization and in vitro studies of chitosan nanoparticles containing androctonus crassicauda scorpion venom', *Journal of Applied Chemical Research*, 7(3), pp. 35–46.
- Dahmane, E.M. *et al.* (2014): 'Extraction and characterization of chitin and chitosan from *Parapenaeus longirostris* from Moroccan local sources', *International Journal of Polymer Analysis and Characterization*, 19(4), pp. 342–351. Available at: <https://doi.org/10.1080/1023666X.2014.902577>.
- Díaz-García, A. and Varela, D. (2020) 'Voltage-Gated K⁺/Na⁺ channels and scorpion venom toxins in cancer', *Frontiers in Pharmacology*. 11(13), 1-11 Available at: <https://doi.org/10.3389/fphar.2020.00913>.
- Elrayess, R.A. *et al.* (2022): 'Scorpion venom antimicrobial peptides induce caspase-1 dependant pyroptotic cell death', *Frontiers in Pharmacology*, 12, pp. 1-10. Available at: <https://doi.org/10.3389/fphar.2021.788874>.
- Fernando, L.D. *et al.* (2021): 'Structural polymorphism of chitin and chitosan in fungal cell walls from solid-state NMR and principal component analysis', *Frontiers in Molecular Biosciences*, 8(August), pp. 1–12. Available at: <https://doi.org/10.3389/fmolb.2021.727053>.
- Firouzeh, N. *et al.* (2021): 'Lethal in vitro effects of optimized chitosan nanoparticles against protozoa of *Echinococcus granulosus*', *Journal of Bioactive and Compatible Polymers*, 36(3), pp. 237–248. Available at: <https://doi.org/10.1177/08839115211014219>.
- Gan, Q. and Wang, T. (2007): 'Chitosan nanoparticle as protein delivery carrier-Systematic examination of fabrication conditions for efficient loading and release', *Colloids and Surfaces B: Biointerfaces*, 59 (1), pp. 24–34. Available at: <https://doi.org/10.1016/j.colsurfb.2007.04.009>.
- Gan, Q. *et al.* (2005): 'Modulation of surface charge, particle size and morphological properties of chitosan-TPP nanoparticles intended for gene delivery', *Colloids*

- and Surfaces B: *Biointerfaces*, 44 (2–3) pp. 65–73. Available at: <https://doi.org/10.1016/j.colsurfb.2005.06.001>.
- Gopakumar, D.A. *et al.* (2018): *Nanomaterials-State of Art, New Challenges, and Opportunities, Nanoscale Materials in Water Purification*. Elsevier Inc. 1-24. Available at: <https://doi.org/10.1016/B978-0-12-813926-4.00001-X>.
- Gopalakrishnakone, P. *et al.* (2015): ‘Scorpion venoms’, *Scorpion Venoms, first ed, Springer*, pp. 1–575. Available at: <https://doi.org/10.1007/978-94-007-6404-0>.
- Hajji, S. *et al.* (2014) ‘Structural differences between chitin and chitosan extracted from three different marine sources’, *International Journal of Biological Macromolecules*, 65, pp. 298–306. Available at: <https://doi.org/10.1016/j.ijbiomac.2014.01.045>.
- Hao, G. *et al.* (2021): ‘Physicochemical characteristics of chitosan from swimming crab (*Portunus trituberculatus*) shells prepared by subcritical water pretreatment’, *Scientific Reports*, 11(1), pp. 1–9. Available at: <https://doi.org/10.1038/s41598-021-81318-0>.
- Hassan, M.I., Mohamed, A.F. and Taher, F.A. (2016): ‘Antimicrobial Activities of Chitosan Nanoparticles Prepared from *Lucilia Cuprina* Maggots (Diptera: Calliphoridae)’, *Journal of the Egyptian Society of Parasitology*, 46(3), pp. 563–570. Available at: <https://doi.org/10.12816/0033977>.
- Heller, A. *et al.* (2013): ‘Engineering of blended nanoparticle platform for delivery of mitochondria-acting therapeutics’, *Journal of Controlled Release*, 4(1), pp. 16288–16293. Available at: <https://doi.org/10.1073/pnas.1210096109>.
- Islam, S., Bhuiyan, M.A.R. and Islam, M.N. (2017): ‘Chitin and Chitosan: Structure, Properties and Applications in Biomedical Engineering’, *Journal of Polymers and the Environment*, 25(3), pp. 854–866. Available at: <https://doi.org/10.1007/s10924-016-0865-5>.
- Jang, M.K. *et al.* (2004): ‘Physicochemical characterization of α -chitin, β -chitin, and γ -chitin separated from natural resources’, *Journal of Polymer Science, Part A: Polymer Chemistry*, 42(14), pp. 3423-3432. Available at: <https://doi.org/10.1002/pola.20176>.
- Jayakumar, R. *et al.* (2010): ‘Biomedical applications of chitin and chitosan-based nanomaterials - A short review’, *Carbohydrate Polymers*, 82(2), pp. 227–232. Available at: <https://doi.org/10.1016/j.carbpol.2010.04.074>.
- Kaya, M., Asan-Ozusaglam, M. and Erdogan, S. (2016): ‘Comparison of antimicrobial activities of newly obtained low molecular weight scorpion chitosan and medium molecular weight commercial chitosan’, *Journal of Bioscience and Bioengineering*, 121(6), pp. 678–684. Available at: <https://doi.org/10.1016/j.jbiosc.2015.11.005>.
- Kellersztein, I. *et al.* (2019): ‘The exoskeleton of scorpions’ pincers: Structure and micro-mechanical properties’, *Acta Biomaterialia*, 94, pp. 565–573. Available at: <https://doi.org/10.1016/j.actbio.2019.06.036>.
- Khan, Ibrahim, Saeed, K. and Khan, Idrees (2019): ‘Nanoparticles: Properties, applications and toxicities’, *Arabian Journal of Chemistry*, 12(7), pp. 908–931. Available at: <https://doi.org/10.1016/j.arabjc.2017.05.011>.
- Küçükgülmez, A. (2018): ‘Extraction of chitin from crayfish (*Astacus leptodactylus*) shell waste’, *Alinteri Ziraat Bilimler Dergisi*, 33(1), pp. 99–104. Available at: <https://doi.org/10.28955/alinterizbd.432139>.
- Laka, M. and Chernyavskaya, S. (2006): ‘Preparation of chitosan powder and investigation of its properties’, *Proceedings of the Estonian Academy of Sciences Chemistry*, 55(2), pp. 78–84.

- Lazaridou, M. *et al.* (2020): 'Formulation and in-vitro characterization of chitosan-nanoparticles loaded with the iron chelator deferoxamine mesylate (DFO)', *Pharmaceutics*, 12(3). 1-17. Available at: <https://doi.org/10.3390/pharmaceutics12030238>.
- M, R. (2017): 'Chitosan as promising materials for biomedical application: review', *Research & Development in Material Science*, 2(4), pp. 170–185. Available at: <https://doi.org/10.31031/rdms.2017.02.000543>.
- Maeda, Y. and Kimura, Y. (2004): 'Antitumor effects of various low-molecular-weight chitosans are due to increased natural killer activity of intestinal intraepithelial lymphocytes in sarcoma 180-bearing mice.', *The Journal of nutrition*, 134(4), pp. 945–950. Available at: <https://doi.org/10.1093/jn/134.4.945>.
- Mirzaei, F. *et al.* (2017): 'A new approach to antivenom preparation using chitosan nanoparticles containing echiscarinatus venom as a novel antigen delivery system', *Iranian Journal of Pharmaceutical Research*, 16(3), pp. 858–867. Available at: <https://doi.org/10.22037/ijpr.2017.2092>.
- Mishal, R. *et al.* (2013): 'Anti-Cancerous Applications of Scorpion Venom', *International Journal of Biological and Pharmaceutical Research*, 4(5), pp. 356-360.
- Mohammadpour Dounighi, N. *et al.* (2012): 'Preparation and in vitro characterization of chitosan nanoparticles containing Mesobuthus eupeus scorpion venom as an antigen delivery system', *Journal of Venomous Animals and Toxins Including Tropical Diseases*, 18(1), pp. 44–52. Available at: <https://doi.org/10.1590/s1678-91992012000100006>.
- Muzzarelli, R.A.A. (2012): 'Chemical and Technological Advances in Chitins and Chitosans Useful for the Formulation of Biopharmaceuticals', *Chitosan-Based Systems for Biopharmaceuticals: Delivery, Targeting and Polymer Therapeutics, first ed, Wiley*, pp. 1–21. Available at: <https://doi.org/10.1002/9781119962977.ch1>.
- Ortiz, E. *et al.* (2015): 'Scorpion venom components as potential candidates for drug development', *Toxicon*, 93, pp. 125–135. Available at: <https://doi.org/10.1016/j.toxicon.2014.11.233>.
- Ou, A. *et al.* (2018): 'The Chemistry of Chitin and Chitosan Justifying their Nanomedical Utilities Biochemistry & Pharmacology: *Open Access the Chemistry of Chitin and Chitosan Justifying their Nanomedical Utilities*', (April). 7, pp. 1-6 Available at: <https://doi.org/10.4172/2167-0501.1000241>.
- Rashidi, G. *et al.* (2016): 'An in vitro study on cytotoxic effects of Androctonus crassicauda Scorpion Venom on K562 Cell Line', *Research Journal of Pharmaceutical, Biological and Chemical Sciences*, 7(6), pp. 846–852.
- Ravi Kumar, M.N.V. (2000): 'A review of chitin and chitosan applications', *Reactive and Functional Polymers*, 46(1), pp. 1–27. Available at: [https://doi.org/10.1016/S1381-5148\(00\)00038-9](https://doi.org/10.1016/S1381-5148(00)00038-9).
- Rebbouh, F., Martin-Eauclaire, M.F. and Laraba-Djebari, F. (2020): 'Chitosan nanoparticles as a delivery platform for neurotoxin II from Androctonus australis hector scorpion venom: Assessment of toxicity and immunogenicity', *Acta Tropica*, 205(December 2019), pp. 1-9. Available at: <https://doi.org/10.1016/j.actatropica.2020.105353>.
- Roy, J.C. *et al.* (2017): 'Solubility of Chitin: Solvents, Solution Behaviors and Their Related Mechanisms', *Solubility of Polysaccharides, first ed, InTech*. 109-127. Available at: <https://doi.org/10.5772/intechopen.71385>.

- Sagheer, F.A.A. *et al.* (2009) 'Extraction and characterization of chitin and chitosan from marine sources in Arabian Gulf', *Carbohydrate Polymers*, 77 (2), pp. 410-419. Available at: <https://doi.org/10.1016/j.carbpol.2009.01.032>.
- Saleh, M. *et al.* (2017) 'Zoogeographical analysis of the egyptian scorpion fauna', *Al-Azhar Bulletin of Science*, 28(1), pp. 1-14. Available at: <https://doi.org/10.21608/absb.2017.8163>.
- Salem, M.L. *et al.* (2016): 'In vitro and in vivo antitumor effects of the Egyptian scorpion *Androctonus amoreuxi* venom in an Ehrlich ascites tumor model', *Springer Plus*, 5(1), pp. 1–12. Available at: <https://doi.org/10.1186/s40064-016-2269-3>.
- Sari, K. *et al.* (2019): 'Effect of milling time on microstructures of nano-sized chitosan', *Journal of Physics: Conference Series*, 1170(1), pp. 1-5. Available at: <https://doi.org/10.1088/1742-6596/1170/1/012058>.
- Shah, P.T. *et al.* (2018): 'Scorpion venom: A poison or a medicine-mini review', *Indian Journal of Geo-Marine Sciences*, 47(4), pp. 773–778.
- Sivanesan, I. *et al.* (2021): 'Reviewing chitin/chitosan nanofibers and associated nanocomposites and their attained medical milestones', *Polymers*, 13(14), pp. 1–17. Available at: <https://doi.org/10.3390/polym13142330>.
- Soon, C.Y. *et al.* (2018): 'Extraction and physicochemical characterization of chitin and chitosan from *Zophobas morio* larvae in varying sodium hydroxide concentration', *International Journal of Biological Macromolecules*, 108, pp. 135–142. Available at: <https://doi.org/10.1016/j.ijbiomac.2017.11.138>.
- Srinivasan, H., Kanayairam, V. and Ravichandran, R. (2018): 'Chitin and chitosan preparation from shrimp shells *Penaeus monodon* and its human ovarian cancer cell line, PA-1', *International Journal of Biological Macromolecules*, 107(PartA), pp. 662–667. Available at: <https://doi.org/10.1016/j.ijbiomac.2017.09.035>.
- Taher, F.A. *et al.* (2019): 'Anti-proliferative effect of chitosan nanoparticles (extracted from crayfish *Procambarus clarkii*, Crustacea: Cambaridae) against MDA-MB-231 and SK-BR-3 human breast cancer cell lines', *International Journal of Biological Macromolecules*, 126, pp. 478–487. Available at: <https://doi.org/10.1016/j.ijbiomac.2018.12.151>.
- Tobassum, S. *et al.* (2018) 'Nature and applications of scorpion venom: an overview', *Toxin Reviews*, 39(3), pp. 214–225. Available at: <https://doi.org/10.1080/15569543.2018.1530681>.
- Zhang, W. *et al.* (2012) 'Physicochemical and structural characteristics of chitosan nanopowders prepared by ultrafine milling', *Carbohydrate Polymers*, 87(1), pp. 309–313. Available at: <https://doi.org/10.1016/j.carbpol.2011.07.057>.
- Zhao, D. *et al.* (2018) 'Biomedical applications of chitosan and its derivative nanoparticles', *Polymers*, 10(4), pp. 1-17. Available at: <https://doi.org/10.3390/polym10040462>.

ARABIC SUMMARY

1- تحضير وتوصيف وكفاءة تحميل سم عقرب الليورس كوينكسترياتس على جزيئات الكيتوزان النانوية المستخلصة من بعض العقارب

مصطفى عبد الحفيظ الشيخ* , أحمد البدرى* , محمد عبد العال* , أحمد عبد العزيز*
* قسم علم الحيوان , كلية العلوم بنين , جامعة الازهر, القاهرة, مصر

الهدف من هذه الدراسة هو استخراج الكيتوزان من بعض العنكبليات ومعرفة بعض خصائصه لدراسته مستقبلا ومعرفة تأثيره في بعض التطبيقات الطبية والصناعية.
تم استخراج جزيئات الكيتين والكيتوزان (الشيتوزان) والكيتوزان النانوية من ثلاثة عقارب في مصر:
amoureuxi . *Androctonus* و *Androctonus crassicauda* (AC) و *Leiurus: quinquestriatus* (LQ) (AA) وقد أظهرت النتائج ارتفاع نسبة الكيتين في العقرب LQ مقارنة بالاثنتين الأخرين. تم إجراء توصيف الكيتين عن طريق اختبار الذوبانية والتحليل الطيفي للأشعة تحت الحمراء (FT-IR). تم تحويل الكيتين إلى الكيتوزان عن طريق نزع مجموعات الأسيتيل كما تم تمييز عينات الكيتوزان باستخدام اختبار الذوبانية ، والتحليل الطيفي أيضا FT-IR ، بالإضافة إلى جهد زيتا (Zeta potential) لتحديد فرق الجهد المحتمل بين وسط التشنت المنتقل والثابت المتصل بكل من الجزيئات النانوية والشحنات المشتتة. تم الحصول على جزيئات الكيتوزان النانوية باستخدام تقنية الطحن بالكرات (البلملنج). تم جمع سم العقرب LQ باستخدام التحفيز الكهربائي، وقد تم توصيفه بتقنية FT-IR ، وتم تحميله على عينات الكيتوزان الثلاثة المحضرة عن طريق الهلام الأيوني (Ionic gellation) للحصول على جسيمات الكيتوزان النانوية المحملة بالسم. تم استخدام تقنية FT-IR وتقنية تشتيت الضوء الديناميكي (DLS) لمعرفة حجم الجزيئات النانوية وتوزيعها والذي تم إثباته أيضاً بنتائج المجهر الإلكتروني النافذ (TEM) ومؤشر التشنت المتعدد (PDI) وجهد زيتا (Zeta potential) لتوصيف كل من جزيئات الكيتوزان النانوية المحضرة بالبلملنج وجسيمات الكيتوزان النانوية المحملة بالسم. أكدت تقنية FT-IR نجاح استخلاص الكيتين وتحضير الكيتوزان من الكيتين وكذلك تكوين جزيئات الكيتوزان النانوية المحملة بالسم. بلغت سعة التحميل 76.50%، بينما بلغت كفاءة تحميل السم 87.98% وكل هذه النتائج أثبتت أن سم العقرب تم تحميله بشكل فعال على عينات الكيتوزان. بشكل عام، تم توضيح بعض الخواص الفيزيائية والكيميائية للمركبات المحضرة والتي تجعلها مناسبة للتطبيقات الطبية الحيوية والدوائية.